Properties of Vector Preisach Models

G. R. KAHLER, E DELLA TORRE, *Fellow, IEEE,* and U. D. PATEL, *Member, IEEE*

***Abstract*-- This paper discusses rotational anisotropy and rotational accommodation of magnetic particle tape. These effects have a performance impact during the reading and writing of the recording process. We introduce the reduced vector model as the basis for the computations. Rotational magnetization models must accurately compute the anisotropic characteristics of ellipsoidally magnetizable media. An ellipticity factor is derived for these media that computes the two-dimensional magnetization trajectory for all applied fields. An orientation correction must be applied to the computed rotational magnetization. For isotropic materials, an orientation correction has been developed and presented. For anisotropic materials, an orientation correction is introduced.**

***Index Terms*—Preisach modeling, reduced model, rotational anisotropy, rotational accommodation, rotational orientation.**

I. INTRODUCTION

THIS paper presents three extensions of the vector Preisach model: the reduced vector Preisach model, RVPM, which eliminates the need for a rotational correction in the SVPM, and extension of the orientation correction to anisotropic media, and a technique for handling vector accommodation.

The accurate characterization of magnetic processes requires a vector model of magnetic hysteresis. The classical Preisach model cannot adequately represent vector magnetic processes since it is inherently a scalar model. Several authors have modified the scalar Preisach model to include the vector features of a magnetic medium [1-4]. The Simplified Vector Preisach Model (SVPM) [1] was developed for computing the vector magnetization in response to a vector-applied field.

The SVPM is a coupled-hysteron model that exhibits both the saturation property and the loss property [1]. The vector magnetization is computed from the integration of the product of a state vector and a Preisach function and then performing the rotational correction. The state vector is computed using the selection rules determined by the applied field. The rotational correction term provides the cross-axis coupling effect of applied fields. This cross-axis coupling term makes it impossible to obtain an analytical closed form solution for the magnetic susceptibility.

The Reduced Vector Preisach Model (RVPM) does not require the rotational correction. The developed vector model uses modified selection rules for state vector calculation.

Using this new model as a basis to characterize the medium, measurements and computations of the angle of magnetization for a magnetic particle (MP) tape rotated in an applied field have been made. This anisotropic material is ellipsoidally magnetizeable, that is, when subject to a constant magnitude rotating field has a magnetization trajectory that is nearly elliptical [11]. This model has an orientation error which has been corrected for isotropic media. We introduce a correction for anisotropic media.

An ellipticity factor has been computed for ellipsoidally anisotropic media that accurately computes the two-dimensional magnetization for large applied fields (50% greater than the hard axis coercivity of the material). A procedure has been derived and is presented for computing the magnetization trajectories for small applied fields. The measured magnetization trajectories (polar plots of the magnetization magnitude and angle) of elliptically magnetizable material changes shape from ellipses for small-applied fields to circles for large applied fields. The measured ellipticity factor, λ, for rotational applied fields approaches one asymptotically as the applied field increases and the magnetization trajectories become circles.

The phenomenon of accommodation has been presented and discussed for scalar Preisach models [9] and a scalar differential equation model has been introduced [10] to compute accommodation. Rotational magnetization measurements have demonstrated vector accommodation for ellipsoidally magnetizable media [11]. From the magnetization trajectories, accommodation is demonstrated for 360° of rotation. The radial change in a magnetization trajectory from the start to the end of applied field rotation is a measure of the accommodation. As the rotating applied field increases, the magnetization trajectories start with shapes of ellipses and exponentially approach the shape of a circle.

II. SIMPLIFIED VECTOR PREISACH MODEL

The SVPM computes the normalized irreversible magnetization components as the product of the rotational correction $R(I_x, I_y, I_z)$, and the basic Preisach integrals I_j,

$$m_{Ij} = R(I_x, I_y, I_z) I_j, \text{ for } j = x, y, \text{ or } z. \quad (1)$$

The output from the basic Preisach integrals I_j are computed as

$$I_j = \iint_{v_j<u_j} Q_j p(u_j, v_j) du_j dv_j, \text{ for } j = x, y, \text{ or } z, \quad (2)$$

where the up and down switching fields are u_j and v_j, the normalized Preisach function is p, and the state function is Q_j. The state function Q_j is determined by selection rules. These

Manuscript received February 4, 2004.

G. R. Kahler and E. Della Torre are with the Institute for Magnetics Research, The George Washington University, Ashburn, VA 20147-2604, USA. E-mail: grkahler@aol.com and edt@gwu.edu.

Umesh D. Patel is with the Goddard Space Flight Center, Greenbelt, MD 20771USA (telephone:301-286-7892, e-mail: upatel@pop500.gsfc.nasa.gov).

selection rules are summarized in Table I for the 2-D model and are generalized for the 3-D model in Table III.

The rotational correction is given by

$$R(I_x, I_y, I_z) = \frac{|I_x| + |I_y| + |I_z|}{\sqrt{I_x^2 + I_y^2 + I_z^2}} \quad (3)$$

It was shown [1] that for any set of values of I_j, the rotation correction ensures the correct magnitude of the magnetization and $1 \le R \le \sqrt{3}$.

The normalized irreversible magnetization is computed as the vector sum of three basic Preisach models as

$$\mathrm{m_I} = \boldsymbol{R}\mathrm{I}. \quad (4)$$

The irreversible magnetization can be computed as the vector sum

$$\mathrm{M_I} = \boldsymbol{M_S}\mathrm{S} \bullet \mathrm{m_I}, \quad (5)$$

where M_s is the saturation magnetization and S is the material squareness matrix defined as

$$\mathrm{S} = \begin{bmatrix} S_x & 0 & 0 \\ 0 & S_y & 0 \\ 0 & 0 & S_z \end{bmatrix}. \quad (6)$$

Thus, to simulate anisotropic media, this model can allow different values for the *S's* along each of the axes and parameters in the basic Preisach models.

The normalized reversible magnetization components can be computed as

$$m_{Rj} = a_{j+} f(H_j) - a_{j-} f(-H_j), \text{ for } j = x, y, \text{ or } z, \quad (7)$$

where the $a_{j\pm}$ variables can be implemented with either a state-independent, magnetization-dependent, or state-dependent reversible magnetization as in the case of the scalar models. The non-linear function $f(H_j)$ is defined as

$$f(H_j) = 1 - e^{-\xi H_j}, \quad (8)$$

where ξ is a model parameter that needs to be identified.

The reversible magnetization can be computed as a vector sum,

$$M_R = (1 - S) M_S m_R, \quad (9)$$

where S is the squareness matrix defined in (6).

Then the total magnetization can be expressed as

$$M_T = M_I + M_R. \quad (10)$$

III. Reduced Vector Preisach Model

The Reduced Vector Preisach Model computes the normalized irreversible magnetization components using the basic Preisach integrals

$$m_{Ij} = \iint_{v_j < u_j} Q_{Rj} p(u_j, v_j) du_j dv_j, \text{ for } j = x, y, \text{ or } z, \quad (11)$$

where the up and down switching fields are u_j and v_j, the normalized Preisach function is p, and the state function is Q_{Rj}.

The state vector, Q_{Rj}, for the RVPM differs from Q_j for the SVPM, and is computed by new selection rules summarized in Table I for the 2-D case. These rules differ from the SVPM case only at the corners. The subscript d is used for the direction in which Q_d is being computed. The subscript c is used to indicate the cross direction. The new selection rules are defined such that no rotational correction is required for computing the magnetization [5].

Similarly, the irreversible magnetization, the reversible magnetization component and the total magnetization are computed using (5), (9) and (10) respectively.

The application of selection rules shown in Table II shows that at any point on the Preisach hyperplane, the sum of the square of the Cartesian components of the state vector obeys

$$Q_x^2 + Q_y^2 + Q_z^2 = 1. \quad (12)$$

For the ellipsoidal magnetization behavior, the major remanence path must satisfy

$$m_{Ix}^2 + m_{Iy}^2 + m_{Iz}^2 = 1. \quad (13)$$

For sufficiently strong fields, the normalized reversible magnetization satisfies

$$m_{Rx}^2 + m_{Ry}^2 + m_{Rz}^2 = 1. \quad (14)$$

Therefore, the normalized total magnetization can be expressed as

$$m_{Tx}^2 + m_{Ty}^2 + m_{Tz}^2 = 1. \quad (15)$$

The important properties of the RVPM can be summarized as:

- The model is applicable to anisotropic media as well as isotropic media.
- The model reduces to the scalar model when the applied field and the initial magnetization lie along only one of the principal axes, whereby, the vector model will have all the properties of the scalar moving model.

In the presence of large fields, the normalized irreversible magnetization and the reversible magnetization each trace out ellipses whose major axes are at right angle to each other for both isotropic and anisotropic media.

IV. Reduced Vector Preisach Model Simulations

The RVPM is applied to an isotropic magnetic medium. For an isotropic medium, values for σ_i and σ_k are equal, and negligible compared to the average critical field $\overline{H_k}$. The material parameters used for simulations are: $\sigma_i = \sigma_k = 165$, $\overline{H_k} = 633, S = 0.57, M_S = 0.014127, \alpha = 33332.81, \xi = 0.0009$.

Simulations were carried out for the orthogonal component H_R of the applied field of $1.1\overline{h_k}$, $1.4\overline{h_k}$ and $4\overline{h_k}$. The vector DOK model [7] is implemented based on the RVPM using the cobweb method [6] for computation speed. Figure 1 shows the magnetization angle versus the applied field angle. It can be seen that the magnetization ratchets as the applied field rotates. For very large applied fields, the magnetization angle becomes equal to the applied field angle for all values.

Figure 2 shows the locus of the magnetization as the applied field is rotated. It is seen that as the field increases, the curves become rounder. The flattening of the loci close to 135° and

315° is a discretization error caused by the jump in the magnetization angle for the respective applied fields.

For isotropic media, since the magnetization rotates faster than the applied field, the rotations of the magnetization need to be corrected using the correction rules defined in [8]. Applying these corrections for the applied fields as in Fig. 1, the corrected magnetization angle vs. applied field angle is plotted as shown in Fig. 3. Figure 4 shows the magnetization loci with corrections for an applied field rotation of 360°. It is seen that the curves are more rounded.

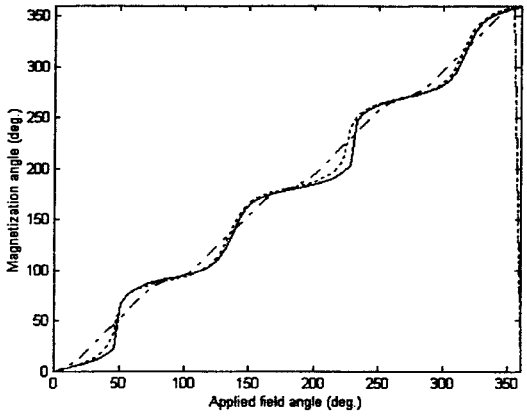

Fig. 1. Magnetization angle vs. applied field angle for applied fields of $1.1\overline{h_k}$ (solid line), $1.4\overline{h_k}$ (dotted line), and $4\overline{h_k}$ (dash-dot line).

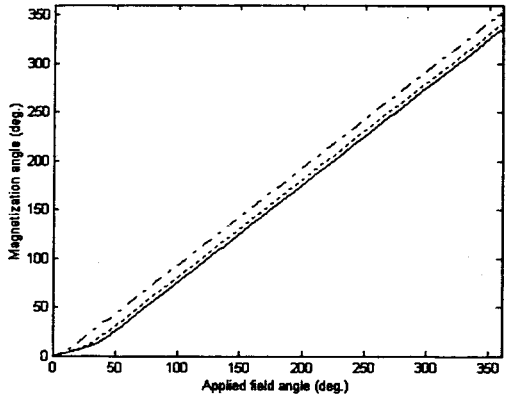

Fig. 2. A plot of the corrected magnetization angle vs. applied field angle for the same conditions as in Fig. 1.

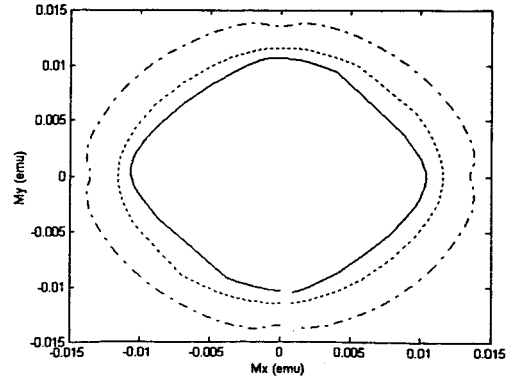

Fig. 3. Locus of magnetization for the same set of applied field rotations as shown in Fig. 1.

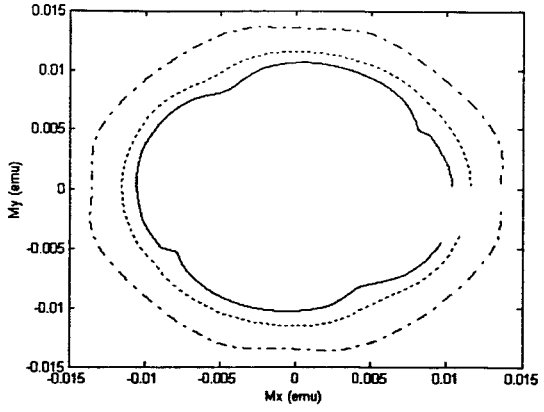

Fig. 4. A plot of the corrected magnetization angle vs. applied field angle for the same conditions as in Fig. 1.

V. Orientation

A simplified vector model was introduced [3] that is the basis for the isotropic model. Two orthogonal Preisach planes, each with its own Preisach function, are defined. For the easy axis Preisach function, seven Preisach parameters (saturation magnetization, squareness, average critical field, zero field susceptibility, standard deviation of interaction field, standard deviation of critical field, and moving parameter) are identified for the isotropic material. The Preisach parameters used for each orthogonal Preisach plane are set equal to this set of identified parameters, thereby, making the model isotropic. The model then computes the irreversible magnetization incorporating a rotational correction factor. From the irreversible magnetization, the reversible magnetization is computed. The irreversible and reversible magnetizations are vectorally added together to obtain the total two-dimensional magnetization. This isotropic computation contains an orientation error as shown in Fig. 1. For isotropic material, the magnetization should follow the applied field after the magnetization begins to rotate. Applying the orientation correction [2] removes this error as shown in Fig 2. This paper extends the correction from the isotropic model to the anisotropic model.

The two-dimensional vector magnetization of MP tape is computed using a cobweb representation of a two-dimensional Gaussian Preisach function [12] and [6], where the first dimension is the X-Preisach plane and the second dimension is the Y-Preisach plane. Figure 5 shows a cobweb for the X-Preisach plane. Outside the outer ring of the cobweb, the Preisach function is considered to have a negligible value. This Preisach function is defined in each plane using seven Preisach parameters identified for the MP tape in each plane. The process of computing the magnetization for the anisotropic MP tape consists of first computing the isotropic magnetization, applying an isotropic orientation correction to this magnetization, and then applying an anisotropic correction to obtain the anisotropic magnetization.

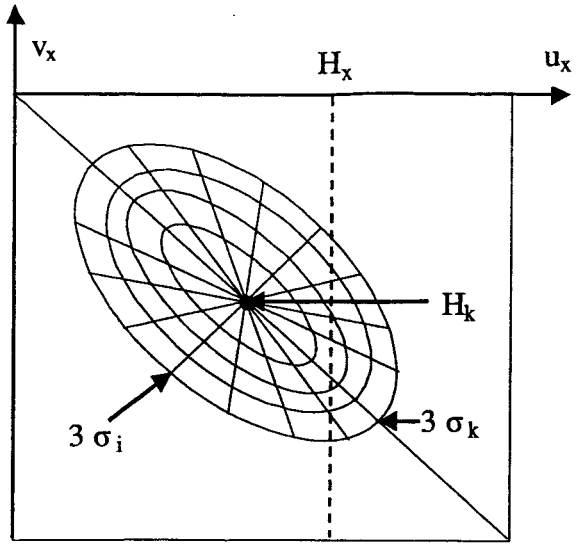

Fig. 5. Cobweb Preisach x-plane centered at the coercivity of a material, H_k. Outer ring of cobweb is assumed to be at least $3\sigma_i$ and $3\sigma_k$ from H_k.

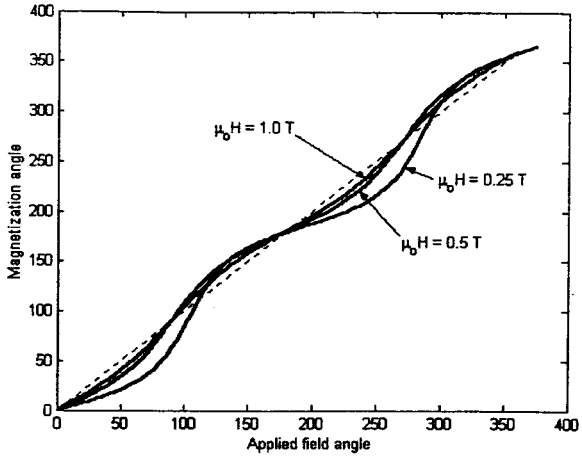

Fig. 6. . MPT computed anisotropic magnetization-applied field angle curves computed from the corrected isotropic magnetization-applied field angle curves. The dotted line is a reference line where the magnetization angle equals the applied field angle.

To compute the isotropic magnetization for the MP tape, the Preisach parameters for the hard axis are set equal to the parameters identified for the easy axis. Using this isotropic model, the isotropic magnetization is computed. Application of the orientation correction removes the orientation error as shown in Fig. 2.

The magnetization-applied field angle curves measured for anisotropic MP tape are double periodic [11] An anisotropic correction factor must be applied to the model results to obtain the double-periodic oscillating characteristic of anisotropic media. Since this oscillating characteristic is sinusoidal in nature, a sinusoidal correction may be derived. Let θ_h be the angle of applied field after applying the orientation correction. Then

$$X = \sin(\theta_h), \tag{16}$$

and

$$Y = \cos(\theta_h) \tag{17}$$

are the sinusoidal representations of the anisotropic applied field, X, and magnetization, Y, respectively. There may be a required linear shift associated with (16) and (17). Let θ_H and θ_M be the anisotropic angles of applied field and magnetization, respectively. Then,

$$\theta_H = X + \Delta\theta_H, \tag{18}$$

and

$$\theta_M = \text{atan}2\left(\frac{\lambda Y}{X}\right) + \Delta\theta_M, \tag{19}$$

where $\Delta\theta_H$ and $\Delta\theta_M$ are the required associated linear shifts, and λ is the anisotropic correction factor. The variables, $\Delta\theta_H$ and $\Delta\theta_M$, respectively, determine the amount of horizontal shift of θ_H and the amount of vertical shift of θ_M. The amplitude of the sinusoidal curve, Y, in (19) is adjusted by λ and generates a double periodic curve between 0° and 360°,

which matches the measured curve, except for applied fields between plus and minus the coercivity, H_C. Figures 6 and 7 show the computed, using (18) and (19), and the measured anisotropic magnetization-applied field angle curves, respectively.

The measured magnetization-applied field curves are computed from measured x- and y-component magnetization for the applied fields μ_0H = 0.5, 0.25, and 1.0 T. The curves are double periodic. The angle of magnetization exceeds the angle of applied field before 180° and before 360° (0°), which correspond to the negative and positive easy-axis directions of the MP tape. This result happens, because the angle of magnetization lies between the easy axis and the angle of applied field. When the x-component of the applied field exceeds the coercivity, H_C, the magnetization tends toward the closest easy axis, resulting

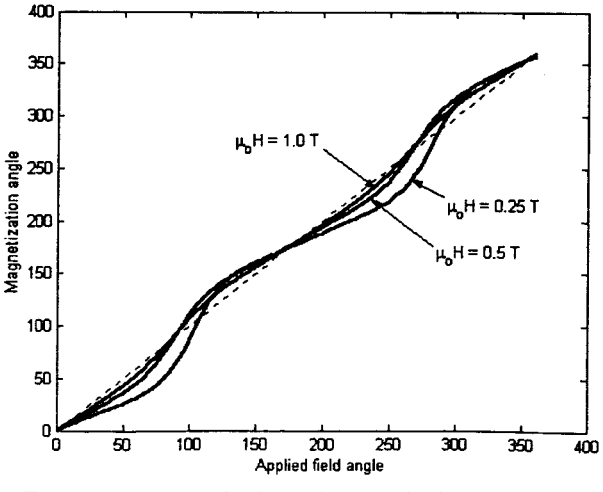

Fig. 7. MPT measured anisotropic magnetization-applied field angle curves for three applied fields. The dotted line is a reference line where the magnetization angle equals the applied field angle.

in a possible angle of magnetization greater than the angle of applied field. As the applied field increases, the curves tend to straighten out and lie along the dashed 45° line, where the angles of magnetization and applied field are equal.

Figure 8 shows the anisotropic correction, λ, used in (19) to adjust the amplitude of the sinusoidal to fit the measured curves in Fig. 7. This curve is a smooth ascending curve to H_C. Above H_C, this curve is a smooth descending curve approaching the value of one asymptotically as the applied field increases. The flat appearance of this curve in the neighborhood of H_C is due to the discretation size of the applied field, $\mu_o H = 0.05$ T.

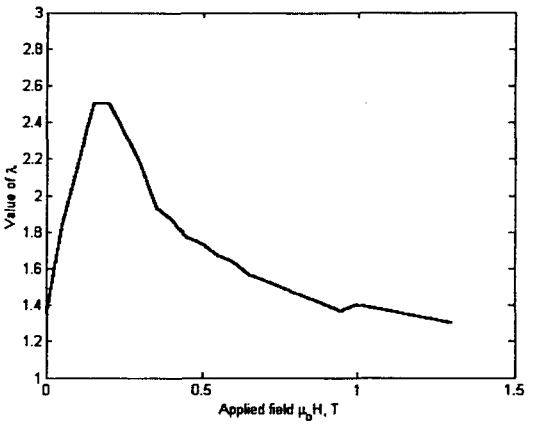

Fig. 8. Measured ellipticity factor for MP tape over the applied field range $H = 0$ T to 1.3 T.

VI. Orientation Extension

The SVPM and the RVPM each produce a magnetization angle-applied field angle curve with a four-fold periodicity as shown in Fig. 1. Since the angle of magnetization actually follows the angle of applied field uniformly, an orientation correction factor is applied by the model to ensure that this characteristic is correctly produced. The orientation correction factor removes the four-fold periodicity from 0° to 360°, but it also removes the two-fold anisotropic periodicity that is characteristic of anisotropic media shown in Fig. 7.

As the applied field increases from zero, the magnetization starts and remains at zero until the applied field begins to sweep through the media's hard-axis Preisach function. At this point, the magnetization begins to rotate and follow the applied field. As the applied field continues to rotate, the magnetization continues to rotate as more hysterons switch.

Because the media are anisotropic, the hysterons along the easy axis of the media switch easier than the hysterons along the hard axis switch, thereby introducing a sinusoidal periodicity into the magnetization. The magnetization always lies between the applied field and the easy axis. Rotating the applied field from 0° to 360°, the magnetization follows the applied field until the easy-axis component of the magnetization switches from positive to negative. When the easy-axis component of the magnetization becomes negative, the magnetization lies between the applied field and the negative easy axis (180°); the magnetization now leads the applied field as shown in Fig. 7. The magnetization leads the applied field until the easy-axis component of the applied field becomes negative, and the magnetization returns to follow the applied field.

To implement a two-dimensional rotational anisotropic model, one must consider how much of the hard axis Preisach function is swept by the applied field as shown in Fig. 9 for a positive applied field. In Fig. 9, the black area of the Preisach function is the area swept by the applied field. When the applied field is less than the Preisach function, none of the Preisach function is swept, and the Preisach function in Fig. 9 is all white. When the applied field is greater than the Preisach function, the entire Preisach function in Fig. 9 is black. The areas of the Preisach function that are black correspond to magnetic particle whose magnetization rotates, whereas, the white areas correspond to magnetization that

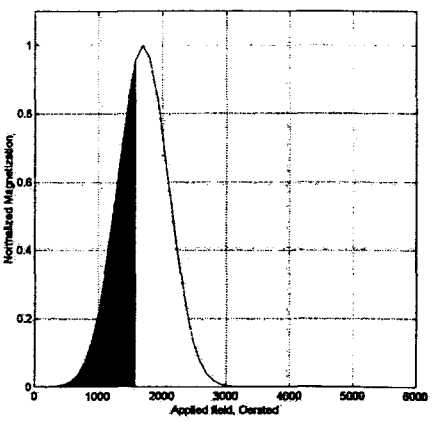

Fig. 9. Preisach function along hard axis of MP tape with applied field, $\mu_o H = 0.15$ T. Magnetization rotates in black area; magnetization oscillates in white area as the applied field rotates.

oscillates. Because the hard axis applied field varies from positive to negative during rotation of 360°, there is a similar sweeping of the hard axis Preisach function for negative applied fields.

The computation of anisotropic magnetization follows the process depicted by the flow diagram shown in Fig. 10. When the applied field does not sweep the Preisach function, $P_R = 0$, there is no rotation of the magnetization, and the magnetization is computed by the RVPM without an ellipticity correction. When the applied field completely sweeps the Preisach function, $P_R = 1$, there is complete rotation of the magnetization, and an ellipticity correction is applied to the entire RVPM computed magnetization. When the Preisach function is partially swept by the applied field, $0 < P_R < 1$, a portion of the magnetization is rotating, C_R, and a portion of the magnetization is oscillating, C_O. The

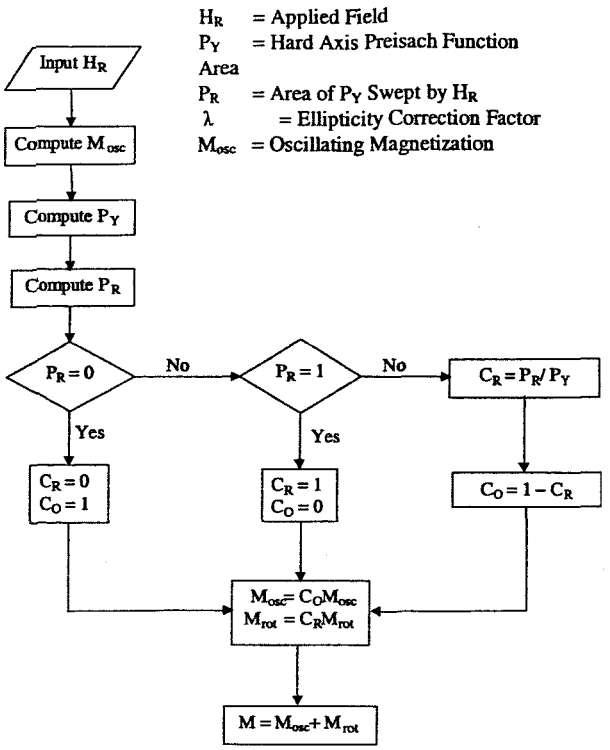

Fig. 10. Flow chart to compute rotating and oscillating magnetization.

oscillating magnetization is computed by multiplying the RVPM magnetization by the coefficient, C_O. The rotating magnetization is computed by multiplying the RVPM magnetization by the ellipticity correction factor and then by the coefficient, C_R. The total magnetization is then determined by vectorally adding the oscillation magnetization and the rotational magnetization as shown in Fig. 11.

VII. Ellipticity Factor

The ellipticity factor is the ratio of the change in magnetization along the easy axis to the change in magnetization along the hard axis. Let H_R be the magnitude of the rotating field. Let M_{ix} be the component

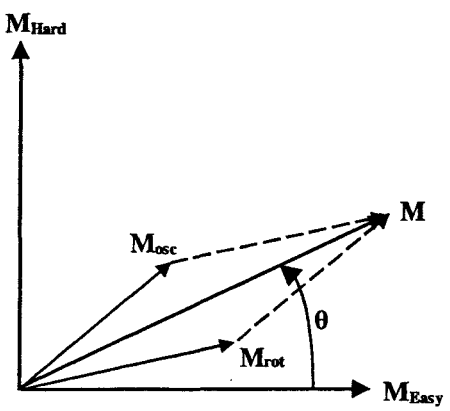

Fig. 11. Vector sum of magnetization contributed by oscillating magnetization (M_{osc}) and magnetization contributed by rotating magnetization (M_{rot}).

of the easy-axis (x-axis) irreversible magnetization and M_{iy} be the component of the hard-axis (y-axis) irreversible magnetization during rotation of the applied field Then

$$M_{ix} = M_S S_x \operatorname{erf}\left(\frac{H_{Rx} - H_{Cx}}{\sigma_x}\right), \tag{20}$$

and

$$M_{iy} = M_S S_y \operatorname{erf}\left(\frac{H_{Ry} - H_{Cy}}{\sigma_y}\right), \tag{21}$$

where M_S is the saturation magnetization, S_x and S_y are the easy and hard axis squareness respectively, H_{Rx} and H_{Ry} are the easy and hard axis average critical fields respectively, and σ_x and σ_y are the easy and hard axis standard deviation of the interaction and critical fields respectively. Define the reversible magnetization function,

$$G = a_+ f(H_R) - a_- f(-H_R) \tag{22}$$

The coefficients, a_+ and a_- in (22) are derived for the easy and hard axes using the irreversible magnetization of (20) and (21),

$$a_{x+} = \frac{1 + M_{ix}}{2} \quad \text{and} \quad a_{x-} = \frac{1 - M_{ix}}{2} \tag{23}$$

and

$$a_{y+} = \frac{1 + M_{iy}}{2} \quad \text{and} \quad a_{y-} = \frac{1 - M_{iy}}{2} \tag{24}$$

The reversible function, f in (22), may be any convenient function that goes through zero when the applied field equals zero and is finite for large values of applied field. Consider the function

$$f(H) = 1 - \exp(-\xi H) \quad \text{for } H > 0 \tag{25}$$

and

$$f(H) = H \quad \text{for } H \le 0. \tag{26}$$

where ξ is a model parameter that needs to be identified. The reversible magnetization is

$$M_R = G(1 - S) H_R M_S \mathbf{1}_{\mathbf{H_R}}, \tag{27}$$

where $\mathbf{1}_{\mathbf{H_R}}$ is a unit vector in the direction of $\mathbf{H_R}$. For the easy and hard axes (x and y respectively),

$$M_{Rx} = G_x (1 - S_x) M_S \tag{28}$$

and

$$M_{Ry} = G_y (1 - S_y) M_S. \tag{29}$$

Adding (20) and (23)

$$M_x = M_S S_x \operatorname{erf}\left(\frac{H_{Rx} - H_{Cx}}{\sigma_x}\right) + G_x (1 - S_x) M_S. \tag{30}$$

Adding (21) and (24)

$$M_y = M_S S_y \operatorname{erf}\left(\frac{H_{Ry} - H_{Cy}}{\sigma_y}\right) + G_y (1 - S_y) M_S. \tag{31}$$

Then, the ellipticity correction factor, λ_e, equals (30) divided by (31)

$$\lambda_e = \frac{S_x \operatorname{erf}\left(\frac{H_{Rx} - H_{Cx}}{\sigma_x}\right) + G_x(1 - S_x)}{S_y \operatorname{erf}\left(\frac{H_{Ry} - H_{Cy}}{\sigma_y}\right) + G_y(1 - S_y)}. \quad (32)$$

The rotational magnetization is computed from

$$M_{rot} = \sqrt{M_x^2 + M_y^2} \quad (33)$$

and when added to M_{osc} computes the resultant magnetization, M. Multiplying (30) by C_o and (31) by C_r enables the computation of θ_H and θ_M, the angle of applied field and the angle of magnetization respectively for the rotation of the applied field. Figure 12 shows the rotation coefficient, C_r, for positive applied fields.

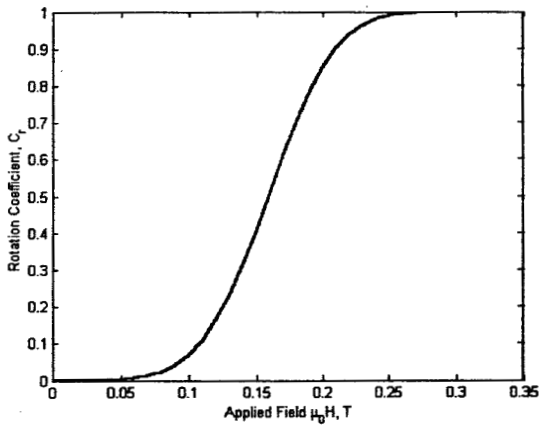

Fig. 12 Computed rotation coefficient, C_r, for positive applied fields.

VIII. Rotational Accommodation

Accommodation, based upon the magnetic interaction between hysterons, causes the drifting of minor loops with the reversal of applied fields. This drifting has an important impact, because it affects the repeatability of the recording process and causes performance changes during the operation of motors and transformers. To understand accommodation, one must understand to where the magnetization is drifting. A magnetic calculation in a complex process will give a wrong answer with the classic Preisach model that does not have accommodation. Accommodation, which is rate independent, appears to be similar to aftereffect, which is rate dependent. Accommodation and aftereffect are caused by different processes.

Vector measurements made on MP tape have displayed vector accommodation [11]. For these measurements, several different applied fields were rotated 360° after initialization of a negative saturation field. The x- and y- components of the magnetization were measured. The vector sum of these measurements, which we call magnetization trajectories, generate elliptic loci [11]. A magnetization trajectory of a material is different for each different applied field. The magnetization trajectories in Fig. 13 are for applied fields with a fixed magnitude and for rotations from 0° to 360°. The difference between the starting and ending magnetization magnitude is a measure of the accommodation. The difference between the starting and ending magnetization angle is a measure of the lag. As the applied field increases, the shape of the trajectories changes exponentially from ellipses to circles as shown in Fig. 13.

The details of the lag angle and the accommodation are shown in Fig. 14 for a measured magnetization MPT trajectory for a clockwise rotating applied field of 0.2 T. A

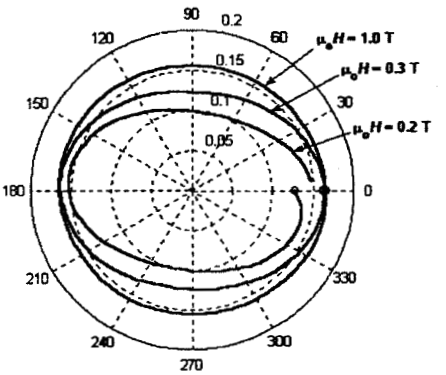

Fig. 13. Change in magnetization for applied fields of μ_0H = 0.2 T, 0.3 T, and 1.0 T

more precise measure of accommodation is computing the difference between starting and ending of the trajectory magnitude after the ending magnetization is extrapolated to the same angle that the magnetization started (0° and 360°).

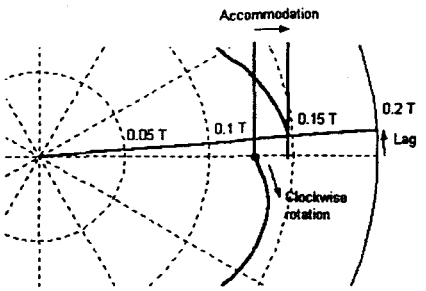

Fig. 14. Measured MPT magnetization trajectory for a clockwise rotating applied field of 0.2 T showing a measure of magnetization accommodation and lag.

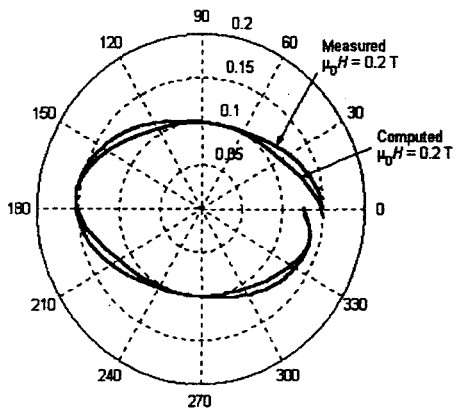

Fig.15. Measured and Computed Ellipsoidal Trajectory at $\mu_0 H = 0.2$ T

Figure 15 shows the measured MPT magnetization trajectory and a computed ellipse with and exponential decay for a rotating applied field of 0.2 T. The computed trajectory shows that the measured trajectory is ellipsoidal and that the accommodation is an exponential decay of this trajectory. The decay tends towards zero as the applied field increases to large values as shown in Fig. 13.

IX. Conclusions

A simpler vector model is developed that does not require the rotational correction for computation speed. The elimination of the rotational correction makes it possible to implement the differential method, a very effective way to compute the magnetization. The simulation results show that the presented model represents isotropic media accurately. Further refinement of this vector model in terms of speed and accuracy is a topic of further research.

The orientation correction for isotropic material was extended for anisotropic material. This extension consists of identifying rotational and oscillatory magnetization by determining the percentage of the hard axis Preisach function swept by the applied field. The extension corrects the magnetization to produce the anisotropic double fold periodicity. The amplitude of the double fold periodic magnetization tends towards zero as the applied field increases.

Vector measurements made on magnetic particle tape, and anisotropic medium, display vector accommodation, which is especially evident in polar format. For small applied fields, the magnetization trajectories form ellipses that exponentially form circles as the applied field increases to large values. A measure of the accommodation is the difference between the start and the end of a magnetization trajectory. The accommodation may be represented as an exponential decay of an ellipsoidal magnetization trajectory. Incorporation of vector accommodation into a Preisach vector model is the subject of future research.

Acknowledgment

The authors would like to thank the members of the Institute for Magnetics Research and especially Dr. Lawrence H. Bennett and Levent Yanik for many helpful discussions.

References

[1] I.D. Mayergoyz, Mathematical Models of Hysteresis, Springer-Verlag:New York, 1991.
[2] E. Della Torre, Magnetic Hysteresis, IEEE Press: Piscataway, NJ, 1999.
[3] E. Della Torre, "A simplified vector Preisach model," *IEEE Trans. Magn.*, vol. 34, Mar. 1998, pp.495-501.
[4] A. Reimers and E. Della Torre, "Fast Preisach-based Vector Magnetization model," *IEEE Trans. Magn.*, vol. 37, Sept. 2001, pp.3349-3352.
[5] U. Patel, Fast Implementation of Scalar and Vector Preisach Models, D.Sc. Dissertation, The George Washington University, Washington, DC, USA, May 2002.
[6] O. Alejos and E. Della Torre, "Improving numerical simulations of Preisach models for accuracy and speed," *IEEE Trans. Magn.*,vol. 36, Sept. 2000, pp.3857-3866.
[7] E. Della Torre and A. Reimers, "Energy considerations in vector magnetization models," *J. Appl. Phys.*, 89(11), June 2001.
[8] E. Della Torre and A. Reimers, "Isotropic Media and the Simplified Vector Preisach Model," *Physica B.*, vol 306, Dec. 2001, pp 72-77.
[9] E. Della Torre, "A Preisach model for accommodation," *IEEE Trans. Magn.* vol. 30, pp. 2701-2707, Sept. 1994.
[10] E. Della Torre, L. Yanik, A. E. Yarimbiyik, and M. Donahue, "A differential equation accommodation model," submitted to *IEEE Trans. Magn.*
[11] G. R. Kahler and E. Della Torre, "Rotational magnetization measurements on magnetic particle recording tape", *Physica B.*, vol 343, 2004, pp 350-356.
[12] A. Reimers and E. Della Torre, "Implementation of the simplified vector model," *IEEE Trans. Mag.*, vol. 38, pp. 837-840, Mar. 2002.

TABLE I. SVPM STATE FUNCTION VALUES IN TWO DIMENSIONS, Q_x

	$v_x > h_x$	$v_x \le h_x \le u_x$	$h_x > u_x$
$v_y > h_y$	$\frac{h_x - v_x}{\lvert h_x - v_x \rvert + \lvert h_y - v_y \rvert}$	0	$\frac{h_x - u_x}{\lvert h_x - u_x \rvert + \lvert h_y - v_y \rvert}$
$v_y \le h_y \le u_y$	-1	no change	1
$h_y > u_y$	$\frac{h_x - v_x}{\lvert h_x - v_x \rvert + \lvert h_y - v_y \rvert}$	0	$\frac{h_x - u_x}{\lvert h_x - u_x \rvert + \lvert h_y - v_y \rvert}$

TABLE II. RVPM STATE FUNCTION VALUES IN TWO DIMENSIONS, Q_x

	$v_x > h_x$	$v_x \le h_x \le u_x$	$h_x > u_x$
$v_y > h_y$	$\frac{h_x - v_x}{\sqrt{(h_x - v_x)^2 + (h_y - v_y)^2}}$	0	$\frac{h_x - u_x}{\sqrt{(h_x - u_x)^2 + (h_y - v_y)^2}}$
$v_y \le h_y \le u_y$	-1	No change	1
$h_y > u_y$	$\frac{h_x - v_x}{\sqrt{(h_x - v_x)^2 + (h_y - v_y)^2}}$	0	$\frac{h_x - u_x}{\sqrt{(h_x - u_x)^2 + (h_y - v_y)^2}}$

TABLE III. STATE FUNCTION VALUES IN THREE DIMENSIONS, Q_j

Number of violations	Violations	States
0	$v_j \le h_j \le u_j$ holds for $j = x, y$ and z	no change
1	$h_j > u_j$ or $h_j < v_j$	$Q_j = 1$ or $Q_j = -1$ and $Q_i = 0$, $i \ne j$
2	Any two combinations of violations in u or v where the thresholds violated are called t_j and t_k.	$Q_j = \frac{h_j - t_j}{\sqrt{(h_j - t_j)^2 + (h_k - t_k)^2}}$, $Q_k = \frac{h_k - t_k}{\sqrt{(h_j - t_j)^2 + (h_k - t_k)^2}}$ and $Q_i = 0$, $i \ne j, k$
3	Any three combinations of violations in u or v where the thresholds violated are called t_i, t_j and t_k.	$Q_i = \frac{h_i - t_i}{\sqrt{(h_i - t_i)^2 + (h_j - t_j)^2 + (h_k - t_k)^2}}$, $Q_j = \frac{h_j - t_j}{\sqrt{(h_i - t_i)^2 + (h_j - t_j)^2 + (h_k - t_k)^2}}$ and $Q_k = \frac{h_k - t_k}{\sqrt{(h_i - t_i)^2 + (h_j - t_j)^2 + (h_k - t_k)^2}}$